Surv. Math. Ind. (1995) 5: 75–108

Surveys on Mathematics for Industry

Constrained motion problems with applications by nonlinear programming methods

Roland Glowinski, Houston, and **Mats Holmström,** Uppsala

Summary. In this paper methods for solving constrained motion problems are discussed — both finite-dimensional and continuous. Constraints are treated by penalty and augmented Lagrangian methods. The equations of motion are discretized by an implicit time-integration scheme, which has energy-preserving properties. Both holonomic and nonholonomic constraints are considered. For the penalty method we use a time-discretization of the penalty term. Some of the problems treated are as follows: constrained double pendulum, colliding strings, and highly nonlinear beams. Numerical results are presented for all the problems discussed.

AMS Subject Classification: 65K, 65M, 65N30.

Keywords: Constrained motions; Nonlinear elasticity; Augmented Lagrangians; Nonlinear elasto-dynamics.

1 Introduction

Many dynamical problems have some sort of constraint imposed on them. In classical mechanics, dynamical problems including holonomic constraints are often solved by the introduction of generalized coordinates, i.e., using the constraint equations $g(x, t) = 0$ we reduce the set of position variables, x, to a smaller set of generalized coordinates, say x'. Thus we have transformed the original, constrained, dynamical problem in the variables x into an unconstrained problem in the generalized coordinates x'.

This approach of stating the problem in terms of generalized coordinates is not always possible. First of all the more general class of nonholonomic constraints cannot be treated using this method. Examples of nonholonomic constraints are inequality constraints or when the constraints involve the solution of a differential equation. A second case is when the derivation of the generalized coordinates is too complicated and, if carried out, prone to errors in the derivation. A third drawback of using generalized coordinates is that the constraint forces do not appear explicitly as part of the solution to the problem. Lastly the resulting equations of motion are often highly nonlinear which can present numerical problems.

A solution is to state the dynamical problems as minimization problems and reduce the constrained dynamical problems to constrained minimization problems. By posing constrained dynamical problems as constrained minimization problems, we can use the wealth of algorithms developed to solve these last problems.

To solve numerically such constrained dynamical minimization problems, two things are especially important. First we need fast and robust methods to perform the actual constrained minimization. Secondly we need time-discretization schemes

that are stable and able to handle stiff problems. In this section we present three methods for constrained minimization; penalty, Lagrangian and augmented Lagrangian methods. We also present an energy-preserving, implicit, time-discretization scheme.

In this article, the above methods are applied to the solution of several constrained dynamical problems. In Sect. 2 we study the problem of a double pendulum subject to both equality and inequality constraints; actually the problems with equality constraints considered in Sect. 2 are modelled by systems of *differential-algebraic equations* for which efficient solution methods already exist (see, e.g., [8, 11, 14] and the references therein). Section 3 treats the problem of vibrating strings subject to inequality constraints and in Sect. 4 we present the problem of large displacement of nonlinear beams. Section 5 contains some conclusions concerning the methods discussed here.

In [10] the methods discussed here have been applied to a real world problem, namely the simulation of the constrained motion of the Space Shuttle robotic arm (the one which played such an important role in the repair of the Hubble telescope).

1.1 Constrained minimization

In this section we present three methods to solve constrained minimization problems. For clarity, we will discuss only the case of equality-constrained minimization. The methods presented are, with minor changes, also applicable to inequality-constrained problems (see [13]).

The finite-dimensional, equality-constrained, minimization problem to be discussed is

$$\begin{cases} \min\limits_{x} f(x), \\ \text{subject to } g(x) = 0. \end{cases} \tag{1}$$

Here $f(x): \mathbb{R}^n \to \mathbb{R}$ and $g(x): \mathbb{R}^n \to \mathbb{R}^m$ ($m \leq n$). We demand that f and g have Lipschitz continuous second derivatives. Let us denote the solution of problem (1) by x^* (assuming there exists one). For an unconstrained minimization problem a necessary condition for a minimum is $\nabla f(x^*) = 0$. This is not, in general, true for the constrained problem (1) since we also have to satisfy the constraints $g(x^*) = 0$. It can be shown (see, e.g., [5]) that the necessary conditions for a stationary point of our constrained minimization problem (1) are

$$\begin{cases} g(x^*) = 0 \text{ and} \\ \nabla f(x^*) + (\nabla g(x^*))^T \lambda^* = 0. \end{cases} \tag{2}$$

Here $\lambda^* \in \mathbb{R}^m$ is the Lagrange multiplier at the solution.

1.2 Penalty methods

The physical interpretation of the quadratic penalty method is simply the introduction of spring-forces in a mechanical system. By introducing the quadratic penalty

functional associated to the constrained problem (1), defined as

$$f_\varepsilon(x) = f(x) + \frac{1}{2\varepsilon} g(x)^T g(x), \tag{3}$$

where $\varepsilon > 0$ is the penalty constant, we have transformed the constrained minimization problem (1) into the unconstrained minimization problem,

$$\min_{x \in \mathbb{R}^n} f_\varepsilon(x). \tag{4}$$

If $\nabla f_\varepsilon(x)$ is the gradient of f_ε of x this reduces to the problem of solving the nonlinear system $\nabla f_\varepsilon(x) = 0$. The drawback is that we are solving a slightly different problem than the original problem. If we denote the solution to (4) by x_ε^*, it can be shown that $x_\varepsilon^* \to x^*$ when $\varepsilon \to 0$ (as shown in, e.g., [5]). Thus as we decrease the value of the penalty parameter we approach the solution to the original constrained problem (1). A difficulty with the penalty method is that the condition number of the Hessian matrix, $\nabla^2 f_\varepsilon(x)$, for the unconstrained minimization problem (4) goes to infinity as $\varepsilon \to 0$ [5]. We thus have a tradeoff between satisfying the constraints and having a well-conditioned problem when using the penalty method.

1.3 Lagrangian methods

The Lagrangian functional associated to the constrained problem (1) is defined by

$$\mathscr{L}(x, \lambda) = f(x) + \lambda^T g(x). \tag{5}$$

Here $\lambda \in \mathbb{R}^m$ is the Lagrange multiplier of the constrained problem (1). Again, denote by x^* the solution to (1) and by λ^* the associated multiplier. In the following it is assumed that $\nabla g(x^*)$ has full rank, since this guarantees the uniqueness of the Lagrange multiplier. If we differentiate the Lagrangian functional with respect to x we have the following system of nonlinear equations,

$$\begin{cases} \nabla_x \mathscr{L}(x^*, \lambda^*) = 0, \\ g(x^*) = 0. \end{cases} \tag{6}$$

Using the definition of the Lagrangian functional (5), the equation system (6) can be written as

$$\begin{cases} \nabla f(x^*) + (\nabla g(x^*))^T \lambda^* = 0, \\ g(x^*) = 0, \end{cases} \tag{7}$$

which is identical to Eq. (2). Relations (7) go back to Lagrange and are necessary conditions for a solution to the problem (1).

A problem with this method is that, even though the original problem (1) has a solution, the Lagrangian functional (5) can be unbounded, since the Hessian of the Lagrangian functional, $\nabla_{xx}^2 \mathscr{L}(x^*, \lambda^*)$, is not necessarily positive definite. Another problem with the Lagrange multiplier method is that the equation system (6) for the case of time-dependent problems is a set of coupled differential and algebraic equations which can be difficult to solve numerically.

1.4 Augmented Lagrangian methods

The augmented Lagrangian method (sometimes also called the method of multipliers in the literature) can be viewed as a combination of the penalty method and the Lagrangian method. It was introduced as a computational tool in 1969, by Hestenes [9] and Powell [12], as an attempt to solve the difficulties of penalty and Lagrange methods that we have described previously.

The augmented Lagrangian functional associated to the constrained problem (1) is

$$\mathscr{L}_\varepsilon(x, \lambda) = f(x) + g(x)^T\left(\frac{1}{2\varepsilon}g(x) + \lambda\right). \tag{8}$$

The corresponding constrained minimization problem is then

$$\begin{cases} \min\limits_{x} \mathscr{L}_\varepsilon(x, \lambda), \\ \text{subject to } g(x) = 0. \end{cases} \tag{9}$$

It can be shown (see [5]) that there exist $\bar{\varepsilon} > 0$ such that x^* is the unconstrained minimum of the augmented Lagrangian, $\mathscr{L}_\varepsilon(x, \lambda^*)$, for all $\varepsilon < \bar{\varepsilon}$.

Since we do not know λ^*, the Lagrange multiplier at the solution, we have to somehow approximate it. Instead of directly solving problem (9) it is possible to only solve the minimization problem, holding the multipliers fixed, and then update the Lagrange multipliers. This leads to the following family of iterative algorithms.

Algorithm 1. Given $i = 0$ and an initial approximation λ_0, execute the following algorithm:

1. Solve the unconstrained minimization problem,

$$\min_{x \in \mathbb{R}^n} \mathscr{L}_\varepsilon(x, \lambda_i) \to x_i.$$

2. Update the Lagrange multiplier, $\lambda_i \to \lambda_{i+1}$.
3. Have we converged to a solution? If not, set $i = i + 1$ and go to 1.

There are many possible choices for the multiplier update in step 2 in Algorithm 1. In this work we have used the Hestenes–Powell update

$$\lambda_{i+1} = \lambda_i + \frac{1}{\varepsilon}g(x_i), \tag{10}$$

which is classified as a first-order update. Another possibility is to use a second-order update, such as

$$\lambda_{i+1} = \lambda_i + [\nabla g(x)^T(\nabla^2_{xx}\mathscr{L}_\varepsilon(x_i, \lambda_i))^{-1}\nabla g(x)]^{-1}g(x_i). \tag{11}$$

These, and several other Lagrange multiplier update methods, are discussed in a paper by Arora et al. [2].

1.5 A class of linear dynamical systems

The time-discretization schemes and their properties that we will describe in this section were introduced in an article by Dean et al. [4].

The dynamical system to be considered is

$$\begin{cases} M\ddot{x} + Ax + C\dot{x} = f(t), \\ x(0) = x_0,\ \dot{x}(0) = x_1,\ x(t) \in \mathbb{R}^d,\ t \in [0, T], \end{cases} \tag{12}$$

where M, A and C are real $d \times d$ matrices and $T > 0$ is a constant. The matrix M is symmetric and positive definite, A is symmetric and positive semi-definite while C is positive semi-definite. In structural dynamics M is usually denoted as the *mass matrix*, since it is dependent of the mass and inertia of the dynamical system. Similarly A is denoted as the *stiffness matrix* since it represents a force that is linear in x. All three matrices are assumed to be constant in time. The right hand side, $f(t)$, can be viewed as an *external force* or torque and is assumed to be piecewise continuous in time for $0 \leq t \leq T$. As usual, we have the notation

$$\dot{x} = \frac{\mathrm{d}x}{\mathrm{d}t} \quad \text{and} \quad \ddot{x} = \frac{\mathrm{d}^2x}{\mathrm{d}t^2}$$

for the first two time derivatives of the dependent variable x.

1.6 An energy relation

Let $(\cdot,\cdot)$ and $|\cdot|$ denote the standard scalar product of $\mathbb{R}^d$, and the associated norm, respectively. For simplicity let us assume for the rest of this section that $f(t) \equiv 0$. Multiplying Eq. (12) by $\dot{x}$, we obtain

$$(M\ddot{x}, \dot{x}) + (Ax, \dot{x}) + (C\dot{x}, \dot{x}) = 0,$$

$$\Leftrightarrow \frac{1}{2}\frac{\mathrm{d}}{\mathrm{d}t}((M\dot{x}, \dot{x}) + (Ax, x)) = -(C\dot{x}, \dot{x}). \tag{13}$$

If we introduce as energy functional for the system (12), $E(t)$, defined as

$$E(t) = \tfrac{1}{2}((M\dot{x}, \dot{x}) + (Ax, x)), \tag{14}$$

then Eq. (13) implies

$$\dot{E} = -(C\dot{x}, \dot{x}) \leqslant 0, \tag{15}$$

since C is positive semi-definite. This shows that $C\dot{x}$ is a friction term that leads to dissipation of energy in the dynamical system (12) over time. If $C = 0$ we have $\dot{E} = 0$, and the system is thus energy conservative.

1.7 A family of time-discretization schemes

The time-discretization of the dynamical system (12) is done by the following schemes:

$$\begin{cases} M\dfrac{x^{n+1}+x^{n-1}-2x^n}{|\Delta t|^2}+A(\alpha x^{n+1}+(1-2\alpha)x^n+\alpha x^{n-1}) \\ \qquad\qquad +C\dfrac{x^{n+1}-x^{n-1}}{2\Delta t}=f^n, \\ x^0=x_0,\ \dfrac{x^1-x^{-1}}{2\Delta t}=x_1,\ x^n\in\mathbb{R}^d,\ 0\le\alpha\le 1/2, \\ N\Delta t=T,\ n=0,1,2,\ldots,N-1,N. \end{cases} \tag{16}$$

Here $x^n\approx x(n\Delta t)$, $f^n=f(n\Delta t)$, α is a constant and $\Delta t>0$ is the time step. As we can see, both $\ddot{x}$ and $\dot{x}$ are discretized by second-order accurate approximations, while x is discretized by a symmetric, weighted mean value. Observe also that the fictitious point x^{-1} is introduced to make the discrete approximation of the initial velocity x_1 symmetric. Then system (16) reduces to the solution of a positive definite, d-dimensional, linear system at each time step.

1.8 Stability properties

In the following we again assume that $f(t)\equiv 0$. To examine the stability properties of scheme (16), we first derive a discrete version of the energy relation (13) by multiplying equation (16) by the discrete velocity to get

$$\begin{aligned} &\frac{1}{2\Delta t}\left[\left(M_\alpha^{\Delta t}\frac{x^{n+1}-x^n}{\Delta t},\frac{x^{n+1}-x^n}{\Delta t}\right)-\left(M_\alpha^{\Delta t}\frac{x^n-x^{n-1}}{\Delta t},\frac{x^n-x^{n-1}}{\Delta t}\right)\right] \\ &+\frac{1}{2\Delta t}\left[\left(A\frac{x^{n+1}+x^n}{2},\frac{x^{n+1}+x^n}{2}\right)-\left(A\frac{x^n+x^{n-1}}{2},\frac{x^n+x^{n-1}}{2}\right)\right] \\ &=-\left(C\frac{x^{n+1}-x^{n-1}}{2\Delta t},\frac{x^{n+1}-x^{n-1}}{2\Delta t}\right), \end{aligned} \tag{17}$$

which is the discrete counterpart of Eq. (13). Here we have introduced the notation

$$M_\alpha^{\Delta t}=M+|\Delta t|^2(\alpha-\tfrac{1}{4})A. \tag{18}$$

Equation (17) implies that, if we choose $C\equiv 0$, the energy function associated with the discrete system (16) is constant (assuming that $M_\alpha^{\Delta t}$ is positive definite) and equal to

$$E_n=\frac{1}{2}\left[\left(M_\alpha^{\Delta t}\frac{x^{n+1}-x^n}{\Delta t},\frac{x^{n+1}-x^n}{\Delta t}\right)+\left(A\frac{x^{n+1}+x^n}{2},\frac{x^{n+1}+x^n}{2}\right)\right]. \tag{19}$$

We see that the energy term is evaluated at the mid-point in time between $n\Delta t$ and $(n+1)\Delta t$ in the discrete case.

It can now be shown [4] that the time-discretization scheme (16) is stable when

$$M_\alpha^{\Delta t} = (M + |\Delta t|^2(\alpha - \tfrac{1}{4})A) \tag{20}$$

is positive definite. If $\alpha \geq 1/4$ then $M_\alpha^{\Delta t}$ is clearly positive definite and the scheme is thus unconditionally stable. If $0 \leq \alpha < 1/4$ then $M_\alpha^{\Delta t}$ is positive definite if, and only if,

$$((M + |\Delta t|^2(\alpha - \tfrac{1}{4})A)y, y) > 0, \quad \forall y \in \mathbb{R}^d \backslash \{0\}. \tag{21}$$

Since M^{-1} is well defined, this is equivalent to

$$\max_{y \in \mathbb{R}^d \backslash \{0\}} \frac{(M^{-1}Ay, y)}{(y, y)} < \frac{1}{|\Delta t|^2(1/4 - \alpha)}, \tag{22}$$

$$\Rightarrow \Delta t < \frac{2}{\sqrt{\lambda_m(1 - 4\alpha)}}, \tag{23}$$

where λ_m is the largest eigenvalue of $M^{-1}A$. So the scheme is conditionally stable for $0 \leq \alpha < 1/4$, the stability condition being inequality (23). Note that if $\alpha = 1/4$, then $M_\alpha^{\Delta t} = M$ and the energy function for the discrete system (19) is of the same form as the energy function of the continuous system (14).

1.9 A class of nonlinear dynamical systems

In this section we will consider a nonlinear variant of Eq. (12), namely

$$M\ddot{x} + Ax + C\dot{x} + \phi(x) = f(t), \quad x(0) = x_0, \ \dot{x}(0) = x_1, \ \phi(x): \mathbb{R}^d \to \mathbb{R}^d \tag{24}$$

where we assume that the nonlinear function ϕ is diagonal, i.e.,

$$\phi(x) = \sum_{i=1}^{d} \phi_i(x_i)e_i, \tag{25}$$

$\{e_i\}_{i=1}^d$ being the standard Euclidean basis in $\mathbb{R}^d$. In the rest of this section, repeated indices do not imply summation. Then $\phi(x)$ is the gradient of a function $V(x)$ defined by the following relations:

$$V(x) = \sum_{i=1}^{d} \Phi_i(x_i), \quad \phi_i(x_i) = \frac{d\Phi_i(x_i)}{dx_i}, \ \Phi_i(x_i) = \int_0^{x_i} \phi_i(\xi)d\xi,$$

$$V(x): \mathbb{R}^d \to \mathbb{R}, \quad \text{and } i = 1, 2, 3, \ldots, d. \tag{26}$$

Taking the derivative of $V(x)$ with respect to time and using Eq. (26), we have by the chain rule the relation

$$\dot{\Phi}_i(x_i) = \frac{d\Phi_i}{dx_i}\frac{dx_i}{dt} = \phi_i(x_i)\dot{x}_i, \quad i = 1, 2, 3, \ldots, d. \tag{27}$$

And we arrive at the relation

$$\phi_i(x_i) = \frac{\dot{\Phi}_i(x_i)}{\dot{x}_i}, \quad i = 1, 2, 3, \ldots, d. \tag{28}$$

Equation (24) can then be written as

$$M\ddot{x} + Ax + C\dot{x} + \left\{\frac{\dot{\Phi}_i(x_i)}{\dot{x}_i}\right\}_{i=1}^{d} = f(t), \quad x(0) = x_0, \ \dot{x}(0) = x_1. \tag{29}$$

To discretize the last term of the left hand side of (29), we use the scheme

$$\frac{\frac{1}{\Delta t}(\Phi_i(x_i^{n+1/2}) - \Phi_i(x_i^{n-1/2}))}{\frac{1}{\Delta t}(x_i^{n+1/2} - x_i^{n-1/2})} = 2\frac{\Phi_i(x_i^{n+1/2}) - \Phi_i(x_i^{n-1/2})}{x_i^{n+1} - x_i^{n-1}}, \quad 0 \le i \le d, \tag{30}$$

where we again have discretized at the midpoints in time,

$$x^{n+1/2} = \frac{x^{n+1} + x^n}{2} \quad \text{and} \quad x^{n-1/2} = \frac{x^n + x^{n-1}}{2}.$$

The discretization of system (24) is then

$$\begin{cases} M\dfrac{x^{n+1} + x^{n-1} - 2x^n}{|\Delta t|^2} + A(\alpha x^{n+1} + (1 - 2\alpha)x^n + \alpha x^{n-1}) \\ \quad + C\dfrac{x^{n+1} - x^{n-1}}{2\Delta t} + 2\left\{\dfrac{\Phi_i(x_i^{n+1/2}) - \Phi_i(x_i^{n-1/2})}{x_i^{n+1} - x_i^{n-1}}\right\}_{i=1}^{d} = f^n, \\ x^0 = x_0, \quad \dfrac{x^1 - x^{-1}}{2\Delta t} = x_1, \ x^n \in \mathbb{R}^d, \ 0 \le \alpha \le 1/2, \\ N\Delta t = T, \ n = 0, 1, 2, \ldots, N-1, N, \ \phi(x): \mathbb{R}^d \to \mathbb{R}^d, \end{cases} \tag{31}$$

i.e., the same time-discretization scheme as (16) with the addition of non-linear terms.

To derive an energy relation for the scheme (31), we multiply by the discrete velocity,

$$\frac{x^{n+1} - x^{n-1}}{2\Delta t},$$

and get the same expression as in the linear case (17), except for the additional potential term

$$\frac{1}{\Delta t}[V(x^{n+1/2}) - V(x^{n-1/2})] \tag{32}$$

in the left hand side. If C and f are zero, we again have constant energy, and the stability of the scheme can be shown under some mild restrictions on $V(x)$. The potential $V(x)$ needs to be bounded from below by some constant $\beta \in \mathbb{R}$, i.e., $V(y) \geq \beta > -\infty, \forall\, y \in \mathbb{R}^d$ ($V(x)$ is then called proper). For such a potential V, it can be shown that the same convergence results holds as in the linear case [4].

2 Double compound pendulum

In this section we will consider the dynamical system of a double compound pendulum subject to inequality and equality constraints, respectively. The inequality constraints are treated by the penalty method while the equality constraints are treated both by a penalty and an augmented Lagrangian method. We present numerical results for both cases.

2.1 Equations of motion for the double pendulum

The motion of a double pendulum is a classical problem in Lagrangian mechanics and often presented as an example of generalized coordinates. There exists no closed form solution since the equations of motion are highly nonlinear. It can be used as a minimal model of a robotic arm, simple in geometry but with complex enough dynamics to make the study of the system interesting.

The geometry of the compound double pendulum that we will consider is shown in Fig. 1. Link 1 is hinged at the origin of the coordinate system, O, and connected to link 2 at joint A. Let subscripts $i = 1, 2$ denote the respective link, then the location of the center of mass, C_i, for a link is determined by the distance a_i. We assume that C_1 is located on the line connecting O and A. The pendulum moves in a fixed plane, so it has two degrees of freedom. Its position is uniquely determined by the two angles $\theta_i = \theta_i(t)$, that each link makes with the x-axis. The inertia of a link with respect to C_i is denoted by I_i and the mass by m_i. We assume a uniform gravity field in the direction of the x-axis with magnitude g.

The equations of motion for the system can then be stated using Lagrange's equations. Since the only force in this system, except for constraint forces, is the uniform gravitational force, the system is conservative and Lagrange's equations are

$$\frac{\mathrm{d}}{\mathrm{d}t}\left(\frac{\partial L}{\partial \dot{\theta}_i}\right) - \frac{\partial L}{\partial \theta_i} = 0, \quad i = 1, 2; \text{ where } L = T - V. \tag{33}$$

Here T denotes the kinetic energy, and V denotes the potential energy of the system.

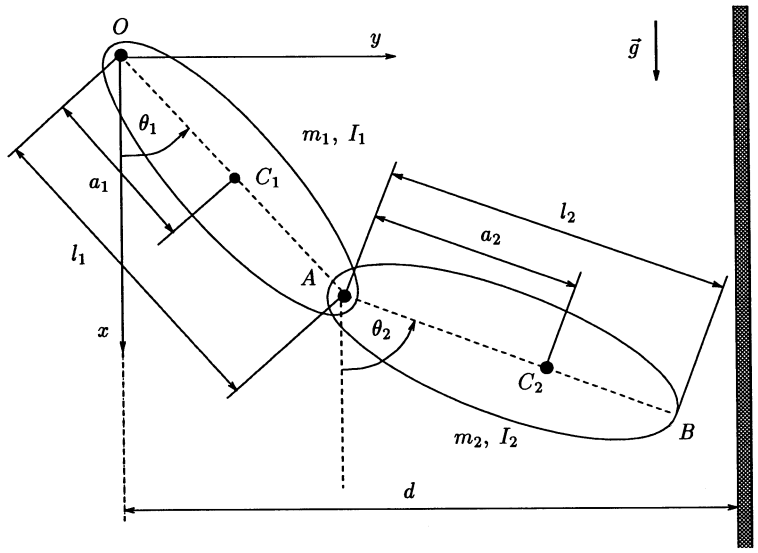

Fig. 1. Geometry of the double compound pendulum

This gives us the two equations of motion, which are

$$\begin{cases} \dfrac{\mathrm{d}}{\mathrm{d}t}[(I_1 + m_1a_1^2 + m_2l_1^2)\dot{\theta}_1 + m_2l_1a_2\dot{\theta}_2\cos(\theta_2 - \theta_1)] \\ \quad - m_2l_1a_2\dot{\theta}_1\dot{\theta}_2\sin(\theta_2 - \theta_1) + g(m_1a_1 + m_2l_1)\sin\theta_1 = 0, \\ \dfrac{\mathrm{d}}{\mathrm{d}t}[(I_2 + m_2a_2^2)\dot{\theta}_2 + m_2l_1a_2\dot{\theta}_1\cos(\theta_2 - \theta_1)] \\ \quad - m_2l_1a_2\dot{\theta}_1\dot{\theta}_2\sin(\theta_2 - \theta_1) + gm_2a_2\sin\theta_2 = 0. \end{cases} \tag{34}$$

As can be seen, the equations of motion (34), are indeed highly nonlinear, due to the presence of the terms $\dot{\theta}_i^2$ and the trigonometric terms in θ_i.

2.2 Inequality constraints

Now we introduce an obstacle in the model, a vertical wall, parallel to the x-axis, at a distance d from the fixed point of the pendulum as shown in Fig. 1. For the moment we assume that only the tip of the pendulum, B, collides with the wall, thus $l_1 < d < l_1 + l_2$. If the wall is rigid, this can be seen as imposing an inequality constraint, $g_B(\theta_1, \theta_2) \leq 0$, on the equations of motion. Since the distance, d, from B to the wall can be written as $d = l_1\sin\theta_1 + l_2\sin\theta_2$, the inequality constraint is $g_B(\theta_1, \theta_2) = l_1\sin\theta_1 + l_2\sin\theta_2 - d \leq 0$.

To solve this constrained motion problem we use the penalty method, described in Sect. 1.2, and introduce the potential energy

$$W_\varepsilon = \frac{1}{2\varepsilon}(g_B(\theta_1, \theta_2)^+)^2, \tag{35}$$

which is the quadratic penalty term. Here the function $(\cdot)^+$ is defined as follows

$$x \in \mathbb{R}, \quad (x)^+ = \begin{cases} x & \text{if } x > 0, \\ 0 & \text{if } x \leq 0. \end{cases} \tag{36}$$

The above discussion has relied on the assumption that only the tip of the pendulum, B, can be in contact with the wall. Including the possibility that the joint A also can interact with the wall is easily done by introducing the additional constraint $g_A(\theta_1, \theta_2) = l_1 \sin\theta_1 - d \leq 0$, which we treat in the same way as we did with the constraint $g_B(\theta_1, \theta_2) \leq 0$. An even more general approach would be to define a function $g_\Omega(\theta_1, \theta_2)$ as

$$g_\Omega(\theta_1, \theta_2) = \max_{p \in \Omega} (x - d)^+, \tag{37}$$

where Ω is the body of the pendulum and p is a point with coordinates (x, y). For simplicity we will only consider the constraint $g_B(\theta_1, \theta_2) \leq 0$ in the following derivations.

Adding W_ε to V in Lagrange's equations (34) we arrive at the following equations of motion for the inequality-constrained system, together with initial conditions for the position and velocity,

$$\begin{cases} \dfrac{\mathrm{d}}{\mathrm{d}t}[(I_1 + m_1 a_1^2 + m_2 l_1^2)\dot\theta_1 + m_2 l_1 a_2 \dot\theta_2 \cos(\theta_2 - \theta_1)] \\ \quad - m_2 l_1 a_2 \dot\theta_1 \dot\theta_2 \sin(\theta_2 - \theta_1) + g(m_1 a_1 + m_2 l_1)\sin\theta_1 \\ \quad + \dfrac{l_1 \cos\theta_1}{\varepsilon}(l_1 \sin\theta_1 + l_2 \sin\theta_2 - d)^+ = 0, \\ \dfrac{\mathrm{d}}{\mathrm{d}t}[(I_2 + m_2 a_2^2)\dot\theta_2 + m_2 l_1 a_2 \dot\theta_1 \cos(\theta_2 - \theta_1)] \\ \quad + m_2 l_1 a_2 \dot\theta_1 \dot\theta_2 \sin(\theta_2 - \theta_1) + g m_2 a_2 \sin\theta_2 \\ \quad + \dfrac{l_2 \cos\theta_2}{\varepsilon}(l_1 \sin\theta_1 + l_2 \sin\theta_2 - d)^+ = 0, \\ \theta_i(0) = \theta_{0i}, \ \dot\theta_i(0) = \theta_{1i}, \ i = 1, 2. \end{cases} \tag{38}$$

The reason for not expanding the time derivative, $\frac{\mathrm{d}}{\mathrm{d}t}(\cdot)$, is that we later want to use that conservation form in the numerical method.

As we can see this is a system of coupled nonlinear differential equations of the form

$$\frac{\mathrm{d}}{\mathrm{d}t} f_j(\theta_i, \dot\theta_i) + g_j(\theta_i, \dot\theta_i) = 0 \quad i, j = 1, 2. \tag{39}$$

To solve it we use the implicit time-integration scheme

$$\begin{cases} \dfrac{1}{\Delta t}\left[f_j\left(\theta_i^{n+1/2}, \dfrac{\theta_i^{n+1}-\theta_i^n}{\Delta t}\right) - f_j\left(\theta_i^{n-1/2}, \dfrac{\theta_i^n-\theta_i^{n-1}}{\Delta t}\right)\right] \\ \quad + \dfrac{1}{2}\left(g_j\left(\theta_i^{n+1/2}, \dfrac{\theta_i^{n+1}-\theta_i^n}{\Delta t}\right) + g_j\left(\theta_i^{n-1/2}, \dfrac{\theta_i^n-\theta_i^{n-1}}{\Delta t}\right)\right) = 0, \\ \theta_i^0 = \theta_{0i},\ n = 1,2,3,\ldots\ i,j = 1,2; \\ \theta_i^1 - \theta_i^{-1} = 2\Delta t\theta_{1i} \text{ and } \theta_i^{n-1}, \theta_i^n \to \theta_i^{n+1}, \end{cases} \tag{40}$$

where $\theta_i(t)$ is approximated by θ_i^n and the velocities $\dot{\theta}_i(t)$ are approximated by

$$\dot{\theta}_i((n-1/2)\Delta t) \approx \frac{\theta_i^n - \theta_i^{n-1}}{\Delta t} \quad \text{and} \quad \dot{\theta}_i((n+1/2)\Delta t) \approx \frac{\theta_i^{n+1} - \theta_i^n}{\Delta t}.$$

Here we have introduced the notation

$$\theta_i^{n+1/2} = \frac{\theta_i^{n+1} + \theta_i^n}{2} \quad \text{and} \quad \theta_i^{n-1/2} = \frac{\theta_i^n + \theta_i^{n-1}}{2}.$$

Again we introduce the fictitious point $-\Delta t$ to approximate the initial velocity $\dot{\theta}_{1i}$.

This scheme is similar to the scheme presented in Sect. 1.7 in that it also uses a midpoint discretization, i.e., we discretize the equations of motion at time $n\Delta t$ by approximating positions and velocities at the times $(n-1/2)\Delta t$ and $(n+1/2)\Delta t$.

2.3 Numerical results

In this section we present some numerical results for the inequality constrained motion of a double pendulum, obtained with the implicit time-integration scheme (40), combined with the penalty method. All the physical parameters are listed in Table 1.

To solve the nonlinear equation system (40) at each time step, Newton's methods was used. We choose to study a single quantity, namely $g_B(\theta_1, \theta_2)$ as a function of time, i.e., the distance from the tip of the pendulum, B, to the rigid wall.

Table 1. Parameter values and initial conditions for the inequality constrained double pendulum

Parameter	Value	Parameter	Value
$\theta_1(0)$	-0.5236 [rad]	$\theta_2(0)$	-1.0472 [rad]
$\dot{\theta}_1(0)$	0 [rad/s]	$\dot{\theta}_2(0)$	0 [rad/s]
a_1	1.63 [m]	a_2	0.99 [m]
l_1	3.26 [m]	l_2	1.98 [m]
m_1	67.1 [kg]	m_2	219 [kg]
I_1	0.8134 [kg × m^2]	I_2	0.8290 [kg × m^2]
d	2.44 [m]	g	9.81 [m/s^2]

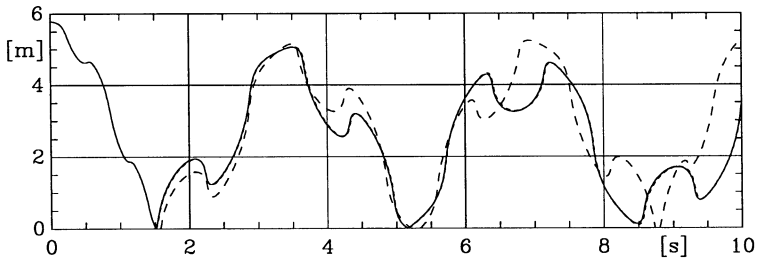

Fig. 2. Distance from the wall to the tip of the pendulum as a function of time for different ε with $\Delta t = 10^{-4}$. Dashed line for $\varepsilon = 10^{-5}$, dotted line for $\varepsilon = 10^{-7}$, and solid line for $\varepsilon = 10^{-9}$. The solid and dotted lines almost coincide with each other

Table 2. The maximum violation of the constraint for different values of ε

ε	Penetration [mm]	Penetration/$(l_1 + l_2)$
10^{-5}	130	0.025
10^{-6}	36	$6.87 \cdot 10^{-3}$
10^{-7}	11	$2.10 \cdot 10^{-3}$
10^{-8}	3.63	$6.93 \cdot 10^{-4}$
10^{-9}	1.16	$2.21 \cdot 10^{-4}$

In Fig. 2, a comparison is made between simulations with different penalty parameters, with the time step fixed. Here the solutions seems to converge when ε is decreased.

In Table 2, the violation of the constraint, or the penetration of the wall, is examined as a function of the penalty constant ε. As can be seen in the last entry of the table, we have to choose $\varepsilon = 10^{-9}$ to reduce the penetration to 10^{-4} of the size of the pendulum. This is an example of the weakness of the penalty method. To satisfy the constraints with high accuracy we have to decrease ε. This can only be done to a certain extent since for small enough ε we will run into accuracy problems due to the finite precision computer calculations, as was noted in Sect. 1.2.

2.4 Equality constraints

In this section we will constrain the motion of the pendulum by an equality constraint. More specifically we constrain the tip of the pendulum, B, to move on a prescribed curve. To make the motion interesting we apply a time-dependent torque, $\tau = \tau(t)$, on the stationary joint, O. The curve we choose to constrain the tip to is an ellipse. The configuration is shown in Fig. 3. Since we now apply a torque, the system is no longer conservative and Lagrange's equations are

$$\frac{\mathrm{d}}{\mathrm{d}t}\left(\frac{\partial L}{\partial \dot{\theta}_i}\right) - \frac{\partial L}{\partial \theta_i} = Q_i, \quad i = 1,2; \text{ where } L = T - V, \tag{41}$$

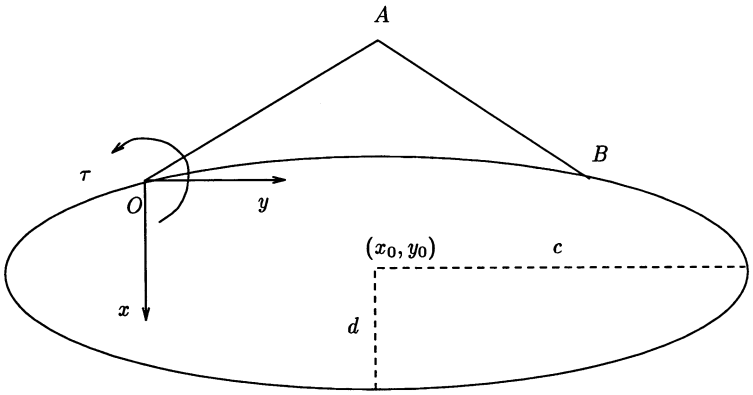

Fig. 3. The geometry of the equality-constrained pendulum

where Q_i are generalized forces corresponding to θ_i. In this case the generalized forces are

$$Q_1 = \tau \quad \text{and} \quad Q_2 = 0. \tag{42}$$

The stationary joint, O, is located on the ellipse. The constraint that the tip, B, is on the ellipse can be stated as

$$\frac{(x_2 - x_0)^2}{c^2} + \frac{(y_2 - y_0)^2}{d^2} = 1, \tag{43}$$

where (x_2, y_2) are the coordinates of the tip of the pendulum, B. We rewrite this in terms of the generalized coordinates as

$$g(\theta_1, \theta_2) = \frac{(l_1 \cos\theta_1 + l_2 \cos\theta_2 - x_0)^2}{c^2} + \frac{(l_1 \sin\theta_1 + l_2 \sin\theta_2 - y_0)^2}{d^2} - 1 = 0, \tag{44}$$

which is the equality constraint on the motion of the pendulum.

For the augmented Lagrangian method we will use the multiplier update algorithm introduced in Sect. 1.4, discretized in time in the same way as we did for the inequality constrained problem (40).

2.5 Numerical results

All parameters used in the numerical experiments are listed in Table 3. The torque we choose to apply is defined by

$$\tau = \tau(t) = \begin{cases} -30 & \text{for } 0 \le t \le 4, \\ 0 & \text{for } t > 4. \end{cases} \tag{45}$$

Table 3. Parameter values and initial conditions for the equality constrained double pendulum

Parameter	Value	Parameter	Value
$\theta_1(0)$	2.271 [rad]	$\theta_2(0)$	0.6591 [rad]
$\dot{\theta}_1(0)$	0 [rad/s]	$\dot{\theta}_2(0)$	0 [rad/s]
a_1	0.5 [m]	a_2	0.25 [m]
l_1	1.0 [m]	l_2	0.5 [m]
m_1	10 [kg]	m_2	5 [kg]
I_1	0.8333 [kg × m^2]	I_2	0.1042 [kg × m^2]
x_0	0.25 [m]	y_0	1 [m]
c	1.155 [m]	d	0.5 [m]
g	9.82 [m/s^2]		

Table 4. Comparison between penalty and augmented Lagrangian methods for the equality-constrained double pendulum

Quantity	Penalty	Augmented Lagrangian
Δt	10^{-6} [s]	$5 \cdot 10^{-4}$ [s]
ε	10^{-6}	10^{-6}
$\max_t \lvert g_B(\theta_1(t), \theta_2(t)) \rvert$	$2.28 \cdot 10^{-4}$	$1.34 \cdot 10^{-5}$
No. of multiplier iterations per time step (mean)	—	40
Total CPU-time (SUN Sparc-2)	56 [min]	3.2 [min]

In Table 4, we list the parameters and results for both the augmented Lagrangian and the penalty methods. As can be seen, the time step is much larger for the augmented Lagrangian. This is because the penalty method failed to converge for larger time steps. Due to this fact, the execution time for the augmented Lagrangian is an order of magnitude faster than the corresponding time for the penalty method, although we have to make approximately 40 multiplier iterations at each time step. Also to be noted is the fact that the maximum penetration is an order of magnitude less in the case of the augmented Lagrangian compared to the penalty solution.

We choose to represent the motion of the pendulum by the y-coordinate of the tip. If we compare the penalty solution with the augmented Lagrangian solution, we can see that they are quite different (Fig. 4). The penalty solution seems damped and smoothed out compared to the augmented Lagrangian solution.

This is even more evident if we examine the total energy of the pendulum, $T + V$, as a function of time. We would expect the energy to have a periodic variation during the four first time units, since we then are applying torque. After four seconds the energy should remain constant, since the torque is zero and therefore the system is conservative. As seen in Fig. 5 the augmented Lagrangian solution approximately satisfies these conditions, while the penalty solution is irregular during the first four seconds, and damped after that.

The conclusion is that the penalty method does not give a satisfactory solution to this equality-constrained problem, neither in terms of accuracy and nor in terms of execution time. The augmented Lagrangian method on the other hand, performs fast with small violations of the constraint.

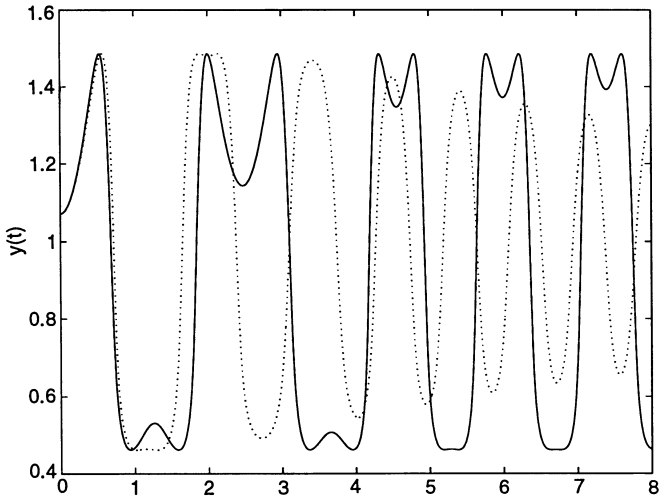

Fig. 4. The y-coordinate for the tip of the pendulum as a function of time. The solid line represents a solution by augmented Lagrangian and the dotted line a solution by penalty

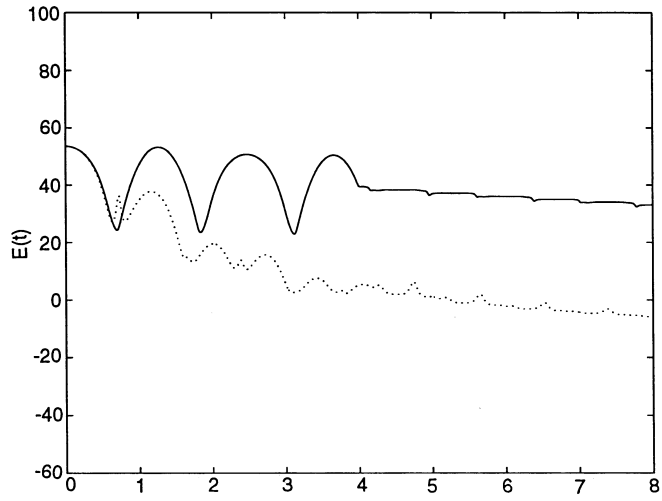

Fig. 5. The total energy of the pendulum $(T + V)$ as a function of time. The solid line represents a solution by augmented Lagrangian and the dotted line a solution by penalty. The energy for the free hanging pendulum is -110.475 for comparison

3 Motion of colliding strings

Consider two strings, U and V, allowed to move in a plane, both with one end fixed at a point A, and the other end fixed at a point B, as shown in Fig. 6.

The strings are not allowed to penetrate each other, that is they do not cross when they collide. Friction forces are neglected, so the collisions are assumed to be elastic. We define an x-axis to coincide with the line from A to B, with $x = 0$

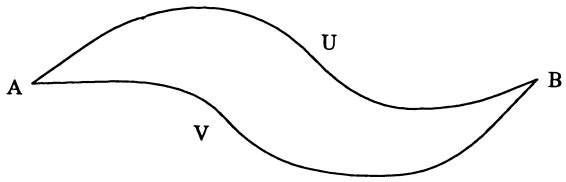

Fig. 6. The configuration of the two strings

corresponding to A and $x = 1$ corresponding to B. The notations we will use for a function $w = w(x, t)$ are as follows:

$$\ddot{w} = \frac{\partial^2 w}{\partial t^2}, \quad \dot{w} = \frac{\partial w}{\partial t}, \quad w_x = \frac{\partial w}{\partial x}, \quad \text{and} \quad w_{xx} = \frac{\partial^2 w}{\partial x^2}.$$

Assuming that the strings' amplitudes of vibration are small compared to unity, we ve the following two wave-equations, coupled by a constraint,

$$\begin{cases} \rho_1 \ddot{u} - \tau_1 u_{xx} = 0, \\ \rho_2 \ddot{v} - \tau_2 v_{xx} = 0, \\ u \geq v, \ u(0, t) = u(1, t) = v(0, t) = v(1, t) = 0, \\ u(x, 0) = u_0, \ v(x, 0) = v_0, \ u_0 > v_0 \ \text{on} \ (0, 1), \\ \dot{u}(x, 0) = u_1, \ \dot{v}(x, 0) = v_1, \\ 0 < x < 1, \ t \geq 0, \end{cases} \tag{46}$$

where $u = u(x, t)$ and $v = v(x, t)$ are the respective displacements of the strings, perpendicular to the x-axis. The parameters ρ_i denote the respective string linear densities and τ_i the tension for $i = 1, 2$. The linear densities and the tension are assumed to be constant for clarity, but the methods that will be presented can easily be modified for nonconstant parameters.

We must choose how to treat the inequality constraint $u \geq v$ in (46). For this problem our approach will be that of penalty with a careful time-discretization of the penalty term. We include the constant in the equations of motion by means of a quadratic penalty function, H_ε, defined as

$$H_\varepsilon(w) = \frac{1}{2\varepsilon}(w^+)^2, \quad H_\varepsilon : \mathbb{R} \to \mathbb{R}, \tag{47}$$

where $\varepsilon > 0$ is the penalty parameter and the function $(\cdot)^+$ was defined earlier in Eq. (36). Taking the derivative of H_ε,

$$H'_\varepsilon(w) = \frac{\mathrm{d}}{\mathrm{d}w} H_\varepsilon(w) = \frac{1}{\varepsilon} w^+, \tag{48}$$

and using this to introduce the penalty function in (46), we have the initial-value problem,

$$\begin{cases} \rho_1 \ddot{u} - \tau_1 u_{xx} = H'_\varepsilon(v-u), \\ \rho_2 \ddot{v} - \tau_2 v_{xx} = -H'_\varepsilon(v-u), \\ u(0,t) = u(1,t) = v(0,t) = v(1,t) = 0, \\ u(x,0) = u_0,\ v(x,0) = v_0,\ u_0 > v_0, \\ \dot{u}(x,0) = u_1,\ \dot{v}(x,0) = v_1, \\ 0 < x < 1,\ t \geq 0, \end{cases} \tag{49}$$

where the constraint, $u \geq v$, now is implicitly contained in the penalty terms $H'_\varepsilon(v-u)$. We now use the same method as in Sect. 1.9, to rewrite a derivative of a potential function, $H'_\varepsilon(v-u)$, as a time derivative by noting that

$$\dot{H}_\varepsilon(v-u) = \frac{\mathrm{d}}{\mathrm{d}t} H_\varepsilon(v-u) = H'_\varepsilon(v-u)(\dot{v}-\dot{u}). \tag{50}$$

Inserting this result in problem (49), we have the initial-value problem

$$\begin{cases} \rho_1 \ddot{u} - \tau_1 u_{xx} = \dfrac{\dot{H}_\varepsilon(v-u)}{\dot{v}-\dot{u}}, \quad \text{or} = 0 \text{ if } \dot{v} = \dot{u}, \\ \rho_2 \ddot{v} - \tau_2 v_{xx} = -\dfrac{\dot{H}_\varepsilon(v-u)}{\dot{v}-\dot{u}}, \quad \text{or} = 0 \text{ if } \dot{v} = \dot{u}, \\ u(0,t) = u(1,t) = v(0,t) = v(1,t) = 0, \\ u(x,0) = u_0,\ v(x,0) = v_0,\ u_0 > v_0, \\ \dot{u}(x,0) = u_1,\ \dot{v}(x,0) = v_1, \\ 0 < x < 1,\ t \geq 0. \end{cases} \tag{51}$$

3.1 Space discretization by a finite element method

We now present a discrete formulation of the initial-value problem. First we discretize problem (51) in space by a finite-element method. To avoid duplication of all the derivations, we will sometimes only consider the formulation for the string $u(x,t)$ but the same applies for $v(x,t)$, unless otherwise stated. We divide the interval $[0,1]$ into I intervals of equal length and define

$$x_i = ih \quad \text{where } h = \frac{1}{I},\ i = 0,1,2,\ldots,I.$$

We also introduce the finite-element space,

$$\mathcal{V}_h = \{v_h \mid v_h \in C^0[0,1],\ v_h|_{[x_i, x_{i+1}]} \in P_1,\ \forall i = 0,1,\ldots,I-1;\ v_h(0) = v_h(1) = 0\},$$

where P_1 is the space of polynomials in one variable of degree ≤ 1. We can note that $\dim \mathscr{V}_h = I - 1$. We also define a vector basis, $\mathscr{B}_h$, of $\mathscr{V}_h$ by

$$\mathscr{B}_h = \{w_i\}_{i=1}^{I-1},\ w_i \in \mathscr{V}_h,\ w_i(x_j) = \delta_{ij},\ \forall j = 0, 1, \ldots, I,\ \forall i = 1, 2, \ldots, I-1.$$

We then can express the elements of $\mathscr{V}_h$ in the basis $\mathscr{B}_h$ by

$$v_h = \sum_{i=1}^{I-1} v_h(x_i) w_i,\ \forall v_h \in \mathscr{V}_h.$$

Now we can construct a finite-element approximation of the continuous problem (49). It follows from (49) that

$$\begin{cases} \rho_1 \int_0^1 \ddot{u} y_h \mathrm{d}x + \tau_1 \int_0^1 u_x y_{hx} \mathrm{d}x - \int_0^1 H_\varepsilon'(v-u) y_h \mathrm{d}x = 0, \\ \forall y_h \in \mathscr{V}_h,\ u(x,0) = u_0,\ \dot{u}(x,0) = u_1,\ t \geq 0. \end{cases} \tag{52}$$

Approximating $u(x, t)$ with $u_h(t)$ in the basis $\mathscr{B}$,

$$u_h(t) = \sum_{j=1}^{I-1} u_h(x_j, t) w_j = \sum_{j=1}^{I-1} u_j(t) w_j,$$

and integrating the second integral by parts, we have

$$\begin{cases} \rho_1 \sum_{j=1}^{I-1} \left(\int_0^1 w_i w_j \mathrm{d}x \right) \ddot{u}_j + \tau_1 \sum_{j=1}^{I-1} \left(\int_0^1 \frac{\mathrm{d}w_i}{\mathrm{d}x} \frac{\mathrm{d}w_j}{\mathrm{d}x} \mathrm{d}x \right) u_j \\ \quad - \int_0^1 H_\varepsilon'(v_h - u_h) w_i \mathrm{d}x = 0, \quad \forall i = 1, 2, 3, \ldots, I-1, \\ u_j(0) = u_{j,0},\ \dot{u}_j(0) = u_{j,1},\ t \geq 0. \end{cases} \tag{53}$$

If we use the trapezoidal rule to evaluate the integrals and calculate the equation for v in the same way, we have (now including v)

$$\begin{cases} \rho_1 \ddot{U}_h + \tau_1 A_h U_h - \left\{ \frac{\dot{H}_\varepsilon(v_i - u_i)}{\dot{v}_i - \dot{u}_i} \right\}_{i=1}^{I-1} = 0, \\ \rho_2 \ddot{V}_h + \tau_2 A_h V_h + \left\{ \frac{\dot{H}_\varepsilon(v_i - u_i)}{\dot{v}_i - \dot{u}_i} \right\}_{i=1}^{I-1} = 0, \\ U_h(0) = U_{0h},\ V_h(0) = V_{0h},\ (U_{0h})_i > (V_{0h})_i, \\ \dot{U}_h(0) = U_{1h},\ \dot{V}_h(0) = V_{1h},\ i = 1, 2, \ldots, I-1, \end{cases} \tag{54}$$

where the penalty term was time-discretized before the integration. Here we have introduced the vectors U_h and V_h, and the matrix A_h, defined as

$$U_h = \begin{pmatrix} u_1 \\ u_2 \\ \vdots \\ u_{I-1} \end{pmatrix} \quad \text{and} \quad A_h = \frac{1}{h^2} \begin{pmatrix} 2 & -1 & & & & & \\ -1 & 2 & -1 & & & 0 & \\ & -1 & 2 & -1 & & & \\ & & & \ddots & & & \\ & & & -1 & 2 & -1 & \\ & 0 & & & -1 & 2 & -1 \\ & & & & & -1 & 2 \end{pmatrix}. \tag{55}$$

The notation for the initial-conditions is

$$U_{0h} = \begin{pmatrix} u_0(h) \\ u_0(2h) \\ \vdots \\ u_0((I-1)h) \end{pmatrix} \quad \text{and} \quad U_{1h} = \begin{pmatrix} u_1(h) \\ u_1(2h) \\ \vdots \\ u_1((I-1)h) \end{pmatrix}. \tag{56}$$

The fact that the mass matrix reduces to the identity matrix when we apply the trapezoidal rule is sometimes called *mass lumping*. If the first integral in Eq. (53) is evaluated by other means then by the trapezoidal rule, e.g., exactly, the mass matrix will be a tri-diagonal matrix.

3.2 Time-discretization by a finite difference scheme

Let us now consider the discretization in time. We introduce the notation

$$u^n \approx u(x, n\Delta t) \quad \text{and} \quad u^{n+1/2} = \frac{u^{n+1} + u^n}{2}, \tag{57}$$

with similar notation for v, and

$$H_\varepsilon^{n+1/2} = H_\varepsilon(v^{n+1/2} - u^{n+1/2}), \tag{58}$$

where $\Delta t > 0$ is the time step and $n = 0, 1, 2, \ldots$ The second order time derivatives, $\ddot{u}$ and $\ddot{v}$, are approximated by the second-order accurate scheme,

$$\ddot{u}(x, n\Delta t) \approx \frac{u^{n+1} + u^{n-1} - 2u^n}{|\Delta t|^2}, \tag{59}$$

the first order time derivatives, $\dot{u}$ and $\dot{v}$, are approximated by the second-order accurate scheme

$$\dot{u}(x, n\Delta t) \approx \frac{u^{n+1} - u^{n-1}}{2\Delta t}, \tag{60}$$

while the second order space derivatives, u_{xx} and v_{xx}, are approximated, in time, by

$$u_{xx}(x, n\Delta t) \approx \alpha u_{xx}^{n+1} + (1 - 2\alpha)u_{xx}^{n} + \alpha u_{xx}^{n-1}, \quad 0 \leq \alpha \leq 1/2, \tag{61}$$

and the penalty term, $\dot{H}_\varepsilon$, is approximated by

$$\dot{H}_\varepsilon(v - u)|_{t = n\Delta t} \approx \frac{H_\varepsilon^{n+1/2} - H_\varepsilon^{n-1/2}}{\Delta t}. \tag{62}$$

The scheme is unconditionally stable (with respect to Δt) for $\alpha \geq 1/4$, as we showed in Sect. 1.5. We have chosen the value 1/4 in our numerical experiments since it has good energy-preserving properties.

We also use the starting procedure

$$\dot{u}(x, 0) \approx \frac{u^1 - u^{-1}}{2\Delta t},$$

where we again have introduced the fictitious point $-\Delta t$.

Using these time-discretizations together with the space-discretization in (54), we have the following solution scheme.

Assume that U_h^0 and U_h^1 are known,
then for $n = 1, 2, 3, \ldots$, with U_h^{n-1}, U_h^n given, compute U_h^{n+1} by solving the following system of nonlinear equations,

$$\begin{cases} \rho_1 \dfrac{U_h^{n+1} + U_h^{n-1} - 2U_h^n}{|\Delta t|^2} - \tau_1 A_h(\alpha U_h^{n+1} + (1 - 2\alpha)U_h^n + \alpha U_h^{n-1}) \\ \quad - \dfrac{1}{\varepsilon}\left\{\dfrac{(v_i^{n+1/2} - u_i^{n+1/2})^{+2} - (v_i^{n-1/2} - u_i^{n-1/2})^{+2}}{(v_i^{n+1} - u_i^{n+1}) - (v_i^{n-1} - u_i^{n-1})}\right\}_{i=1}^{I-1} = 0, \\ \rho_2 \dfrac{V_h^{n+1} + V_h^{n-1} - 2V_h^n}{|\Delta t|^2} - \tau_2 A_h(\alpha V_h^{n+1} + (1 - 2\alpha)V_h^n + \alpha V_h^{n-1}) \\ \quad + \dfrac{1}{\varepsilon}\left\{\dfrac{(v_i^{n+1/2} - u_i^{n+1/2})^{+2} - (v_i^{n-1/2} - u_i^{n-1/2})^{+2}}{(v_i^{n+1} - u_i^{n+1}) - (v_i^{n-1} - u_i^{n-1})}\right\}_{i=1}^{I-1} = 0, \\ U_h^0 = U_{0h},\ V_h^0 = V_{0h},\ (U_{0h})_i > (V_{0h})_i, \\ i = 1, 2, \ldots, I - 1, \end{cases} \tag{63}$$

where U_h^1 is given by solving (63) for $n = 0$ using

$$U_h^{-1} \approx U_h^1 - 2\Delta t U_{1h}, \tag{64}$$

and where the vectors U_h^n and V_h^n are defined as

$$U_h^n = \begin{pmatrix} u_1^n \\ u_2^n \\ \vdots \\ u_{I-1}^n \end{pmatrix}, \tag{65}$$

and A_h, U_{0h}, V_{0h}, U_{1h}, V_{1h} are defined as before in (55) and (56).

The resulting system of equations (63) that has to be solved at each time step is nonlinear with $2(I-1)$ unknowns.

3.3 Numerical results

In this section we will present the result of a numerical experiment with scheme (63). The parameters used in the experiment are as follows:

$$\begin{cases} \rho_1 = \rho_2 = 1, \\ \tau_1 = \tau_2 = 1, \\ \varepsilon = 10^{-6}, \\ \Delta t = 10^{-4}, \\ \alpha = 1/4, \\ I = 100, \end{cases} \tag{66}$$

and the initial conditions are (shown in Fig. 7a)

$$\begin{cases} U_{1h} = V_{1h} = 0, \\ (U_{0h})_i = 0.02\sin(\tau i h), \\ (V_{0h})_i = -0.01\sin(2\pi i h), \\ i = 1, 2, \ldots, I-1. \end{cases} \tag{67}$$

The system of nonlinear equations (63) arising at each time step was solved by Newton's method. The test case solved numerically showed a good performance of the described method using the time-discretized penalty term, although the time step had to be chosen quite small ($\Delta t = 10^{-4}$) to capture the sometimes violent motion of the strings.

At 0.35 time unit (Fig. 7b) the strings collide, and it is interesting to see that, at least from inspection, the strings motion coincide with the motion of two unconstrained strings. We have total symmetry at time 0.5 as shown in Fig. 7c. After 1 time unit the configuration is symmetric with the initial configuration, but V is now the string of maximum displacement.

The maximum penetration (violation of the constraint) was $1.0 \cdot 10^{-5}$ or 0.05% of the maximum displacement for this experiment.

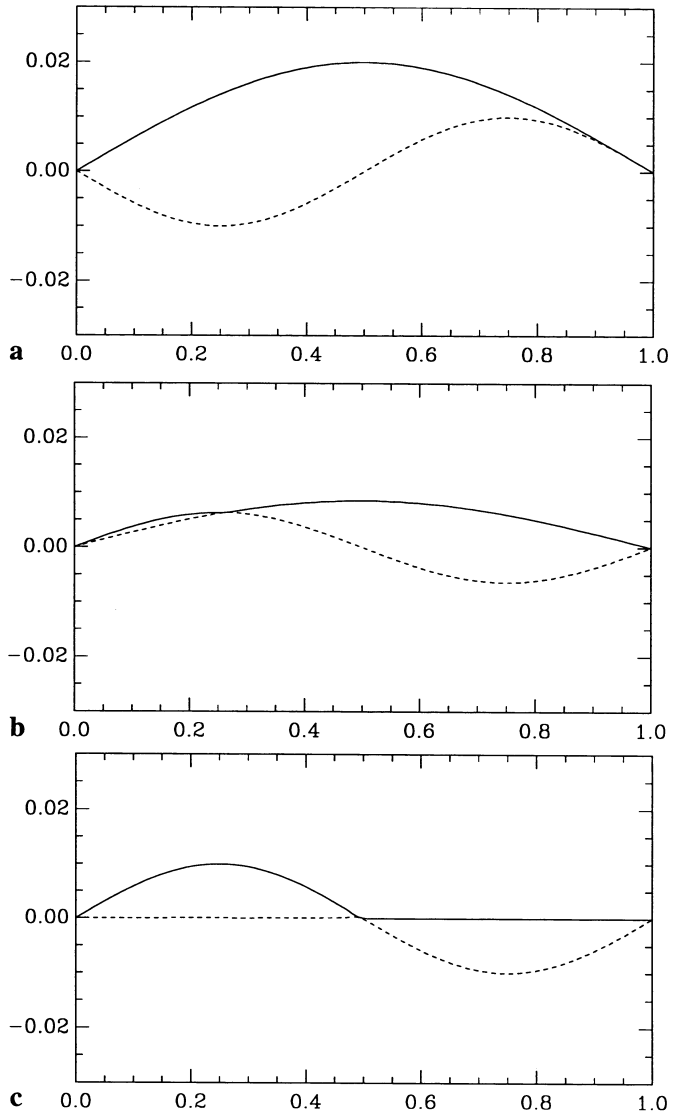

Fig. 7. a The initial configuration. **b** The configuration after 0.36 and **c** after 0.50 time unit. The solid line is the string U, and the dashed line is V. Observe the different scales

4 Large displacement of beams

In this section we will treat the problem of calculating the motion of largely displaced beams. This is an equality-constrained problem where the constraint is that the beam is supposed to be locally inextensible. The theoretical part of the presentation is based on Bourgat et al. [3] and Glowinski and Le Tallec [7], where the authors treat the constraint by an augmented Lagrangian method and use

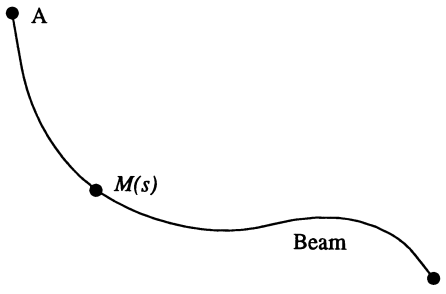

Fig. 8. Sketch of the configuration of the beam

a dissipative Houbolt scheme for the time-integration. In this section we introduce the energy-preserving scheme presented in Sect. 1.5, instead of the Houbolt scheme. We also treat the problem by a time-discretized penalty method in addition to the augmented Lagrangian method.

The theoretical background for the static case is presented in Sect. 4.1 and for the dynamic case in Sect. 4.5.

4.1 Analysis of the static problem

The geometry of the problem is shown in Fig. 8 and the assumptions concerning the mechanical behavior of the beams are as follows:

— torsional effects are neglected,
— the diameters of the beams are small compared to their length L, so that the cross-sections remain undeformed,
— the beams are inextensible, and
— the beams are flexible so that they obey a linear strain-stress relation.

We also introduce the following notation:

— A and B are the extremities of the beam,
— s is the curvilinear abscissa with $s(A) = 0$ and $s(B) = L$, where L is the length of the beam, and
— M(s) is the generic point of the beam with coordinates $\mathbf{x}(s)$.

4.2 Problem formulation

For the static case we can express the total potential energy of the beam J as

$$J(\mathbf{x}) = \frac{1}{2}\int_0^L EI\,|\mathbf{x}''|^2\,\mathrm{d}s - \int_0^L \mathbf{f}\cdot\mathbf{x}\,\mathrm{d}s,\ x\in V, \tag{68}$$

where the first integral represents the flexural (bending) energy and the second integral the potential energy due to external forces. Here $\mathbf{f}$ denotes the linear

density of external forces, EI the flexural stiffness of the beam, and $\mathbf{x}'$ and $\mathbf{x}''$ the first and second derivative of $\mathbf{x}$ with respect to s. We then have to solve the following *local* minimization problem in order to find the stable equilibrium positions for the beam,

$$\min_{x \in V} J(\mathbf{x}), \tag{69}$$

where the set V is defined as

$$V = \{\mathbf{v} \mid \mathbf{v} \in H^2(0, L; \mathbb{R}^3),\ |\mathbf{v}'(s)| = 1 \text{ on } [0, L], \text{ plus boundary conditions}\}. \tag{70}$$

Here $|\mathbf{v}'(s)| = 1$ is the inextensibility condition on the admissible solutions. The Hilbert space $H^2(0, L; \mathbb{R}^3)$ is defined as usual by

$$H^2(0, L; \mathbb{R}^3) = \{\mathbf{v} \mid \mathbf{v}, \mathbf{v}', \mathbf{v}'' \in L^2(0, L; \mathbb{R}^3)\}. \tag{71}$$

The boundary conditions in (70) are that both ends of the beam are fixed in space,

$$\mathbf{x}(0) = \mathbf{x}_A,\ \mathbf{x}(L) = \mathbf{x}_B,\ \mathbf{x}_A, \mathbf{x}_B \in \mathbb{R}^3, \tag{72}$$

or that the ends are fixed and also clamped,

$$\begin{cases} \mathbf{x}(0) = \mathbf{x}_A,\ \mathbf{x}(L) = \mathbf{x}_B,\ \mathbf{x}_A, \mathbf{x}_B \in \mathbb{R}^3, \\ \mathbf{x}'(0) = \mathbf{x}'_A,\ \mathbf{x}'(L) = \mathbf{x}'_B,\ \mathbf{x}'_A, \mathbf{x}'_B \in \mathbb{R}^3,\ |\mathbf{x}'_A| = |\mathbf{x}'_B| = 1, \end{cases} \tag{73}$$

or a combination of (72) and (73).

The minimization problem (69) has a long history. Setting $\mathbf{f} = 0$ gives us Euler's Elastica problem, where for every solution we also have the symmetric solution by reflection in the line from A to B. This is one example of the nonuniqueness of the solutions to (72). If we choose $EI = 0$ and $\mathbf{f}$ constant, the solution is a catenoid curve. Concerning the existence of solutions to the general minimization problem (69), it can be shown [1] that if $|\vec{B} - \vec{A}| < L$, then (69) has at least one solution, that in general is nonunique.

4.3 Penalty method

We will only treat the fixed-end boundary condition (72), the extension to clamped-end boundary conditions (73) is easily made.

Again the idea of the penalty method is to satisfy the inextensibility condition, $|\mathbf{x}'(s)| = 1$, as well as possible by including the quadratic penalty term in the expression for the total potential energy (68). So instead of solving (69), we solve the slightly different problem,

$$\min_{\mathbf{x} \in V_0} J_\varepsilon(\mathbf{x}). \tag{74}$$

Here we have introduced the affine space

$$V_0 = \{\mathbf{v} \mid \mathbf{v} \in H^2(0, L; \mathbb{R}^3),\ \mathbf{v}(0) = \mathbf{x}_A,\ \mathbf{v}(L) = \mathbf{x}_B\}, \tag{75}$$

associated with the boundary conditions (72). The functional J_ε is defined as

$$J_\varepsilon(\mathbf{x}) = \frac{1}{2}\int_0^L EI\,|\mathbf{x}''|^2\,\mathrm{d}s - \int_0^L \mathbf{f}\cdot\mathbf{x}\,\mathrm{d}s + \int_0^L \rho H_\varepsilon(|\mathbf{x}'(s)|^2 - 1)\,\mathrm{d}s, \quad \mathbf{x} \in V_0, \tag{76}$$

where the penalty function, H_ε, is defined as

$$H_\varepsilon(w) = \frac{1}{2\varepsilon}w^2, \quad w \in \mathbb{R}, \tag{77}$$

with $\varepsilon > 0$ being the penalty parameter. Solving for the stationary solutions of (76) by the calculus of variations gives us the following Euler–Lagrange equations

$$\int_0^L EI\mathbf{x}''\cdot\mathbf{y}''\,\mathrm{d}s - \int_0^L \mathbf{f}\cdot\mathbf{y}\,\mathrm{d}s + 2\int_0^L \rho H_\varepsilon'(|\mathbf{x}'(s)|^2 - 1)\mathbf{x}'\cdot\mathbf{y}'\,\mathrm{d}s = 0, \quad \forall\,\mathbf{y} \in \mathrm{d}V_0(\mathbf{x}), \tag{78}$$

where the tangent set, $\mathrm{d}V_0(\mathbf{x})$, of admissible variations is defined as

$$\mathrm{d}V_0(\mathbf{x}) = \{\mathbf{y} \mid \mathbf{y} \in H^2(0, L; \mathbb{R}^3),\ \mathbf{y}(0) = \mathbf{y}(L) = 0\}. \tag{79}$$

In order to solve the problem (78) by finite-element methods, a suitable approximation of $H^2(0, L; \mathbb{R}^3)$ is needed. If we introduce the partition $\{s_i\}_{i=0}^N$ of the beam, such that

$$0 = s_0 < s_1 < s_2 \cdots < s_{i-1} < s_i < s_{i+1} < \cdots < s_I = L$$

then we can approximate $H^2(0, L; \mathbb{R}^3)$ by the finite-dimensional space

$$V_h = \{\mathbf{v}_h \in C^1([0, L]; \mathbb{R}^3) \mid \mathbf{v}_h|_{[s_i, s_{i+1}]} \in \mathbf{P}_3(s_i, s_{i+1})\ \forall\, i \in [0, I-1)\}.$$

Here $\mathbf{v}_h|_{[s_i, s_{i+1}]}$ is the restriction of $\mathbf{v}_h$ to the interval $[s_i, s_{i+1}]$ and $\mathbf{P}_k(s_i, s_{i+1})$ denotes the set of polynomials in s with coefficients in $\mathbb{R}^3$ and of degree less than or equal to k. For future use, it is convenient to also introduce the spaces,

$$V_{0h} = \{\mathbf{v} \in V_h \mid \mathbf{v}(0) = \mathbf{x}_A,\ \mathbf{v}(L) = \mathbf{x}_B\}$$

and

$$\mathrm{d}V_{0h} = \{\mathbf{v} \in V_h \mid \mathbf{v}(0) = \mathbf{v}(L) = 0\}.$$

We have that $V_h \subset H^2(0, L; \mathbb{R}^3)$ and that the dimension of V_{0h} is $6I$. The finite-element representation that V_h corresponds to is said to be of *Hermite cubic* type, and the associated degrees of freedom are

$$\{\mathbf{v}_h(s_i)\}_{i=0}^I \quad \text{and} \quad \{\mathbf{v}_h'(s_i)\}_{i=0}^I.$$

If we assume boundary conditions of the type (72), the finite-dimensional formulation of (78) is

$$\int_0^L EI\mathbf{x}''\cdot\mathbf{y}''\,ds - \int_0^L \mathbf{f}\cdot\mathbf{y}\,ds$$

$$+ 2\int_0^L \rho H_\varepsilon(|\mathbf{x}'(s)|^2 - 1)\mathbf{x}'\cdot\mathbf{y}'\,ds = 0, \quad \forall \mathbf{y}\in dV_{0h},\ \mathbf{x}\in V_{0h}. \tag{80}$$

This is clearly a nonlinear system of equations. To evaluate the integrals in (80), we used Gaussian quadrature.

4.4 Augmented Lagrangian method

Here we will use the augmented Lagrangian method together with a decoupling of the nonlinearity of the inextensibility condition by introducing new variables, coupled to the old ones by linear equalities. Here the natural choice is to define a new variable $\mathbf{p} = \mathbf{x}'$. First we introduce the augmented Lagrangian functional associated with J and the inextensibility constraint as

$$\mathscr{L}_r(\mathbf{y}, \mathbf{q}; \boldsymbol{\mu}) = J(\mathbf{y}) + (\boldsymbol{\mu}, \mathbf{q} - \mathbf{y}') + \frac{1}{2\varepsilon}|\mathbf{q} - \mathbf{y}'|^2, \{\mathbf{y}, \mathbf{q}; \boldsymbol{\mu}\}\in(V\times H)\times H, \tag{81}$$

with the Hilbert space $H = L^2(0, L; \mathbb{R}^3)$ and its usual scalar product $(\cdot,\cdot)$ and norm $|\cdot|$, V is defined as before with the boundary conditions (72), $\varepsilon > 0$ is the penalty parameter, $\boldsymbol{\mu}$ is the Lagrange multiplier function.

Problem (69) can then be stated as the saddle-point problem

$$\begin{cases} \text{Find } \{\mathbf{x}, \mathbf{p}; \boldsymbol{\lambda}\}\in(V\times H)\times H \text{ such that} \\ \mathscr{L}_\varepsilon(\mathbf{x}, \mathbf{p}; \boldsymbol{\mu}) \le \mathscr{L}_\varepsilon(\mathbf{x}, \mathbf{p}; \boldsymbol{\lambda}) \le \mathscr{L}_\varepsilon(\mathbf{y}, \mathbf{q}; \boldsymbol{\lambda}), \\ \forall\ \{\mathbf{y}, \mathbf{q}; \boldsymbol{\mu}\}\in(V\times H)\times H. \end{cases} \tag{82}$$

It can be proved [7] that the solutions to (82) are also solutions to our original problem (69), if (82) is considered as a local saddle-point problem. To solve the problem (82), the following algorithm of Uzawa type ([6]) is used.

Algorithm 2. $\boldsymbol{\lambda}^0\in H$ and $\mathbf{x}^{-1}$ given; then, for $n \ge 0$, $\boldsymbol{\lambda}^n$ and $\mathbf{x}^{n-1}$ being known, determine $\mathbf{p}^n$, $\mathbf{x}^n$, and $\boldsymbol{\lambda}^{n+1}$ successively by

$$\mathscr{L}_\varepsilon(\mathbf{x}^{n-1}, \mathbf{p}^n; \boldsymbol{\lambda}^n) \le \mathscr{L}_\varepsilon(\mathbf{x}^{n-1}, \mathbf{q}; \boldsymbol{\lambda}^n), \quad \forall \mathbf{q}\in H,\ \mathbf{p}^n\in H, \tag{83}$$

$$\mathscr{L}_\varepsilon(\mathbf{x}^n, \mathbf{p}^n; \boldsymbol{\lambda}^n) \le \mathscr{L}_\varepsilon(\mathbf{y}, \mathbf{p}^n; \boldsymbol{\lambda}^n), \quad \forall \mathbf{y}\in V,\ \mathbf{x}^n\in V, \text{ and} \tag{84}$$

$$\boldsymbol{\lambda}^{n+1} = \boldsymbol{\lambda}^n + \rho_n((\mathbf{x}^n)' - \mathbf{p}^n). \tag{85}$$

To obtain $\mathbf{p}^n$ in (83), we have to solve the minimization problem,

$$\min_{|\mathbf{q}|=1} \mathscr{L}_\varepsilon(\mathbf{x}^{n-1}, \mathbf{q}; \boldsymbol{\lambda}^n),$$

and the solution is

$$\mathbf{p}^n = \frac{\mathbf{P}}{|\mathbf{P}|}, \quad \text{where } \mathbf{P}(s) = \lambda^n - \frac{1}{\varepsilon}(\mathbf{x}^{n-1})'. \tag{86}$$

Using the calculus of variation of minimization problem (84) can be stated as the equivalent problem

$$\begin{cases} \text{Find } \mathbf{x}^n \in V \text{ such that} \\ \displaystyle\int_0^L \left[EI(\mathbf{x}^n)'' \cdot \mathbf{y}'' + \frac{1}{\varepsilon}(\mathbf{x}^n)' \cdot \mathbf{y}' \right] ds \\ \quad = \displaystyle\int_0^L \left[\mathbf{f} \cdot \mathbf{y} + \left(\lambda^n + \frac{1}{\varepsilon}\mathbf{p}^n \right) \cdot \mathbf{y}' \right] ds, \quad \forall \mathbf{y} \in dV(\mathbf{x}^n). \end{cases} \tag{87}$$

The finite-element approximation of (87) can be obtained by replacing V with $V \cap V_h$, giving us three, independent, linear systems of order $6I$ (order $6(I-1)$ if we have boundary conditions of type (73)), with the same bandmatrix (bandwidth 7) which is symmetric, positive-definite and independent of I if ε is fixed. That means we only have to do a Cholesky factorization once, thus each iteration consists of solving six sparse, triangular, systems.

4.5 Analysis of the dynamical problem

Here we introduce the following notation:

$$\mathbf{x}(t) = \mathbf{x}(s, t), \ \mathbf{x}' = \frac{\partial \mathbf{x}}{\partial s}, \ \dot{\mathbf{x}} = \frac{\partial \mathbf{x}}{\partial t}, \ \mathbf{x}'' = \frac{\partial^2 \mathbf{x}}{\partial s^2}, \text{ and } \ddot{\mathbf{x}} = \frac{\partial^2 \mathbf{x}}{\partial t^2}.$$

By a virtual work principle ([7]), we have in the continuous case the initial value problem:

Find $\mathbf{x}: [0, T] \to V_t$ such that

$$\begin{cases} \displaystyle\int_0^L \rho \ddot{\mathbf{x}} \cdot \mathbf{y}\, ds + \int_0^L EI\mathbf{x}'' \cdot \mathbf{y}''\, ds - \int_0^L \mathbf{f} \cdot \mathbf{y}\, ds = 0, \\ \forall \mathbf{y} \in dV_t(\mathbf{x}), \ t \in (0, T), \ \mathbf{x}(0) = \mathbf{x}_0, \ \dot{\mathbf{x}}(0) = \mathbf{x}_1. \end{cases} \tag{88}$$

The set V_t is defined by

$$V_t = \{\mathbf{y} \mid \mathbf{y} \in H^2(0, L; \mathbb{R}^3), \ |\mathbf{y}'(s)| = 1 \text{ on } [0, L];$$

$$\mathbf{y}(0) = \mathbf{x}_a(t) \text{ and } \mathbf{y}(L) = \mathbf{x}_b(t)\},$$

and

$$dV_t(\mathbf{x}) = \{\mathbf{y} \mid \mathbf{y} \in H^2(0, L; \mathbb{R}^3),\ \mathbf{x}'(s, t)\cdot\mathbf{y}'(s) = 0 \text{ on } [0, L];$$

$$\mathbf{y}(0) = \mathbf{y}(L) = 0\}.$$

4.6 Penalty method

Applying the penalty method to Eq. (88), we have the initial-value problem:

Find $\mathbf{x}: [0, T] \to V_{0t}$ such that

$$\begin{cases} \displaystyle\int_0^L \rho\ddot{\mathbf{x}}\cdot\mathbf{y}\,ds + \int_0^L EI\mathbf{x}''\cdot\mathbf{y}''\,ds - \int_0^L \mathbf{f}\cdot\mathbf{y}\,ds \\ \quad + 2\displaystyle\int_0^L \rho H_\varepsilon'(|\mathbf{x}'(s)|^2 - 1)\mathbf{x}'\cdot\mathbf{y}'\,ds = 0 \quad \forall\,\mathbf{y}\in dV_{0t}(\mathbf{x}), \\ t\in(0, T),\ \mathbf{x}(0) = \mathbf{x}_0,\ \dot{\mathbf{x}}(0) = \mathbf{x}_1. \end{cases} \tag{89}$$

where

$$H_\varepsilon'(w) = \frac{dH_\varepsilon}{dw}, \quad w\in\mathbb{R}.$$

The set V_{0t} is defined by

$$V_{0t} = \{\mathbf{y} \mid \mathbf{y}\in H^2(0, L; \mathbb{R}^3),\ \mathbf{y}(0) = \mathbf{x}_a(t) \text{ and } \mathbf{y}(L) = \mathbf{x}_b(t)\},$$

and

$$dV_{0t}(\mathbf{x}) = \{\mathbf{y} \mid \mathbf{y}\in H^2(0, L; \mathbb{R}^3),\ \mathbf{y}(0) = \mathbf{y}(L) = 0\}.$$

Again we will use a time-discretization of the penalty term. Taking the time derivative of $H_\varepsilon(|\mathbf{x}'|^2 - 1)$, we have that

$$\frac{\partial}{\partial t}H_\varepsilon(|\mathbf{x}'|^2 - 1) = \dot{H}_\varepsilon(|\mathbf{x}'|^2 - 1) = H_\varepsilon'(|\mathbf{x}'|^2 - 1)2\mathbf{x}'\cdot\dot{\mathbf{x}}'. \tag{90}$$

Using this result in (89), we have the initial-value problem:

Find $\mathbf{x}: [0, T] \to V_t$ such that

$$\begin{cases} \displaystyle\int_0^L \rho\ddot{\mathbf{x}}\cdot\mathbf{y}\,ds + \int_0^L EI\mathbf{x}''\cdot\mathbf{y}''\,ds - \int_0^L \mathbf{f}\cdot\mathbf{y}\,ds \\ \quad + \displaystyle\int_0^L \rho\dot{H}_\varepsilon(|\mathbf{x}'(s)|^2 - 1)\frac{\mathbf{x}'\cdot\mathbf{y}'}{\mathbf{x}'\cdot\dot{\mathbf{x}}'}ds = 0 \quad \forall\,\mathbf{y}\in dV_{0t}(\mathbf{x}), \\ t\in(0, T),\ \mathbf{x}(0) = \mathbf{x}_0,\ \dot{\mathbf{x}}(0) = \mathbf{x}_1. \end{cases} \tag{91}$$

The finite-difference approximations that we use are as follows:

$$\dot{H}_\varepsilon^n \approx \frac{H_\varepsilon^{n+1/2} - H_\varepsilon^{n-1/2}}{\Delta t},$$

$$\ddot{\mathbf{x}}(n\Delta t) \approx \frac{\mathbf{x}^{n+1} + \mathbf{x}^{n-1} - 2\mathbf{x}^n}{|\Delta t|^2},$$

$$\mathbf{x}''(n\Delta t) \approx (\alpha\mathbf{x}^{n+1} + (1-2\alpha)\mathbf{x}^n + \alpha\mathbf{x}^{n-1})'', \quad 0 < \alpha < 1/2, \text{ and}$$

$$\mathbf{x}'(n\Delta t) \approx \frac{(\mathbf{x}^{n+1} + \mathbf{x}^{n-1})'}{2},$$

where

$$\mathbf{x}^n = \mathbf{x}(n\Delta t),\ \mathbf{x}^{n+1/2} = \frac{\mathbf{x}^{n+1} + \mathbf{x}^n}{2},\ H_\varepsilon^{n+1/2} = H_\varepsilon(|\mathbf{x}'((n+1/2)\Delta t)|^2 - 1).$$

Now we can formulate the discrete problem corresponding to (91) as the following sequence of static type problems:

$$\mathbf{x}^j \in V_j \text{ is given for } j = 0, 1;$$

then, for $n \geq 1$, assuming $\mathbf{x}^j \in V_j$ are known for $j = n-1, n$, we obtain $\mathbf{x}^{n+1} \in V_{n+1}$ as the solution of:

Find $\mathbf{x}^{n+1} \in V_{n+1}$ such that

$$\begin{cases} \displaystyle\int_0^L \frac{\rho}{|\Delta t|^2}(\mathbf{x}^{n+1} + \mathbf{x}^{n-1} - 2\mathbf{x}^n)\cdot\mathbf{y}\,ds \\ \quad + \displaystyle\int_0^L EI(\alpha\mathbf{x}^{n+1} + (1-2\alpha)\mathbf{x}^n + \alpha\mathbf{x}^{n-1})''\cdot\mathbf{y}''\,ds - \int_0^L \mathbf{f}\cdot\mathbf{y}\,ds \\ \quad + \displaystyle\int_0^L \rho(H_\varepsilon^{n+1/2} - H_\varepsilon^{n-1/2})\frac{(\mathbf{x}^{n+1} + \mathbf{x}^{n-1})'\cdot\mathbf{y}'}{(\mathbf{x}^{n+1} + \mathbf{x}^{n-1})'\cdot(\mathbf{x}^{n+1} - \mathbf{x}^{n-1})'}\,ds = 0 \\ \forall\,\mathbf{y} \in dV_{n+1}(\mathbf{x}^{n+1}),\ t \in (0, T),\quad \mathbf{x}(0) = \mathbf{x}_0,\ \dot{\mathbf{x}}(0) = \mathbf{x}_1. \end{cases} \tag{93}$$

Here V_{n+1} is V_{0t} at time $(n+1)\Delta t$.

We also need a starting procedure to compute $\mathbf{x}^1$. For that purpose the approximation,

$$\dot{\mathbf{x}}(0) = \mathbf{x}_1 \approx \frac{\mathbf{x}^1 - \mathbf{x}^{-1}}{2\Delta t}, \tag{94}$$

is used, where the fictitious value $\mathbf{x}^{-1} = \mathbf{x}(-\Delta t)$ is introduced. Since $\mathbf{x}^0 = \mathbf{x}_0$ is known and $\mathbf{x}^{-1}$ is given by (94), we can use (93) to compute $\mathbf{x}^1$.

The problem (93) is similar to the static problem treated in Sect. 4.3 and can be solved by identical methods; $\mathbf{x}^0$ is also obtained by the solution of a static problem.

4.7 Numerical experiments

The parameters for the experiment presented below are as follows:

$$\begin{cases} N = 20, \\ \varepsilon = 1.5 \cdot 10^{-4}, \\ L = 32.6\ \text{m}, \\ \mathrm{d}t = 0.01\ \text{s}, \\ EI = 700\ \text{N/m}^2, \\ \rho = 7.67\ \text{kg/m}, \text{ and} \\ \alpha = 1/4. \end{cases} \tag{95}$$

The initial velocity, $\mathbf{x}_1 = 0$, and the boundary conditions are of the type (72), with $\mathbf{x}_a = (0, 0)$ and $\mathbf{x}_b = (20, 0)$ at time $t = 0$. The starting position, $\mathbf{x}_0$, is the equilibrium position corresponding to the boundary conditions, obtained by solving the static problem. For times $t > 0$ the extremity A is held fixed at $\mathbf{x}_a = (0, 0)$, while the other end of the beam B is allowed to fall freely.

As we can see in Fig. 9a during the first five seconds the motion is smooth, but after approximately seven seconds a shock wave is propagating from B to A (Fig. 9b).

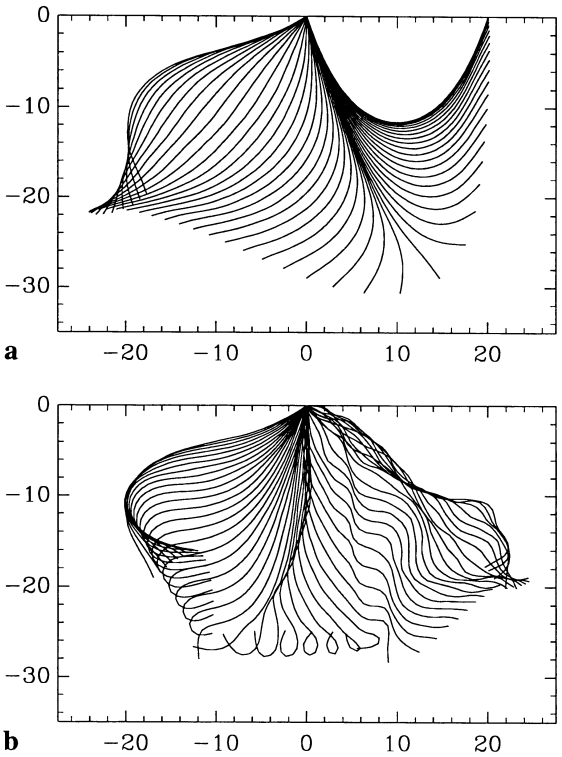

Fig. 9. The motion of the beam **a** for $0 \leq t \leq 5$ and **b** $5 \leq t \leq 10$, with 0.1 s between plots

4.8 *Augmented Lagrangian method*

Again we have the initial-value problem:

Find $\mathbf{x}:[0, T] \to V_t$ such that

$$\begin{cases} \displaystyle\int_0^L \rho\ddot{\mathbf{x}}\cdot\mathbf{y}\,ds + \int_0^L EI\mathbf{x}''\cdot\mathbf{y}''\,ds - \int_0^L \mathbf{f}\cdot\mathbf{y}\,ds = 0 \\ \forall\,\mathbf{y}\in dV_t(\mathbf{x}),\ t\in(0, T),\ \mathbf{x}(0) = \mathbf{x}_0,\ \dot{\mathbf{x}}(0) = \mathbf{x}_1, \end{cases} \tag{96}$$

where V_t and $dV_t(\mathbf{x})$ are defined as before.

Using the same finite-difference approximations as in the penalty case, we can formulate the discrete problem corresponding to (96) as the following sequence of static problems:

$$\mathbf{x}^j\in V_j \text{ is given for } j = 0, 1;$$

then, for $n \geq 1$, assuming $\mathbf{x}^j\in V_j$ are known for $j = n-1, n$, we obtain $\mathbf{x}^{n+1}\in V_{n+1}$ as the solution of

Find $\mathbf{x}^{n+1}\in V_{n+1}$ such that

$$\begin{cases} \displaystyle\int_0^L \frac{\rho}{|\Delta t|^2}(\mathbf{x}^{n+1} + \mathbf{x}^{n-1} - 2\mathbf{x}^n)\cdot\mathbf{y}\,ds \\ \quad + \displaystyle\int_0^L EI(\alpha\mathbf{x}^{n+1} + (1-2\alpha)\mathbf{x}^n + \alpha\mathbf{x}^{n-1})''\cdot\mathbf{y}''\,ds - \int_0^L \mathbf{f}\cdot\mathbf{y}\,ds = 0 \\ \forall\,\mathbf{y}\in dV_{n+1}(\mathbf{x}^{n+1}),\ t\in(0, T),\ \mathbf{x}(0) = \mathbf{x}_0,\ \dot{\mathbf{x}}(0) = \mathbf{x}_1. \end{cases} \tag{97}$$

The starting procedure is the same as for the penalty problem (94).

The problem (97) is similar to the static problem treated earlier and can be solved by identical methods (Algorithm 1).

If $\mathbf{f}$ is dependent on $\mathbf{x}$ we can treat $\mathbf{f}$ explicitly by $\mathbf{f} = \mathbf{f}(\mathbf{x}^n, \mathbf{x}^{n-1})$ to keep the linearity of the Uzawa algorithm.

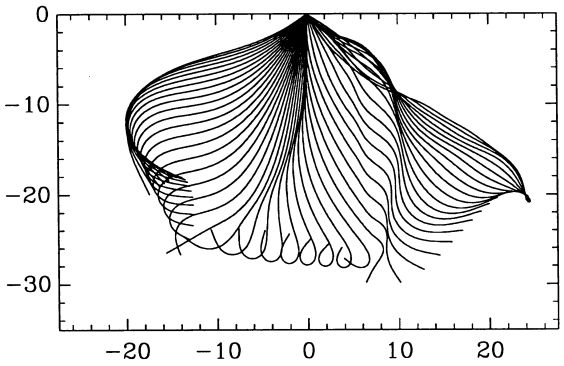

Fig. 10. The motion of the beam for $5 \leq t \leq 10$, with 0.1 s between plots

4.9 Numerical experiments

Here we have the same parameters, boundary conditions and initial conditions as in the problem solved by a penalty method in Sect. 4.7.

In Fig. 10 we can see that the motion is much smoother than for the penalty solution, and the violent motion after seven seconds does not appear.

5 Conclusions

In this work we have presented several methods for solving constrained motion problems and we have applied these methods for the solution of some test problems. An important part has been the implicit time-discretization scheme with energy-preserving properties. This scheme and variations of it have performed well in the numerical experiments and seem suited for the special ability demands of constrained motion problems.

The problem of incorporating the constraints in the equations of motion have been treated by penalty and augmented Lagrangian methods. It was seen that the augmented Lagrangian method is superior to the penalty method in terms of accuracy for all test cases. This does not mean that there are no cases where the penalty method is an acceptable choice. For cases when the motion is smooth, in the sense that the constraint forces are small, the penalty method was seen to perform well. This was especially true for the time-discretized penalty method which seems to increase the stability of the penalty method. Examples of this are the inequality-constrained double pendulum and the problem of two colliding strings. The advantage of the penalty method is its simplicity and speed, although in some cases the need for excessively small time steps for acceptable accuracy of the solution made the penalty method much slower than the augmented Lagrangian method. This was the case for the equality-constrained double pendulum.

The methods presented in this work can be seen as a robust set of tools for the solution of constrained motion problems as have been shown for the various test cases presented. The augmented Lagrangian method combined with the implicit time-discretization scheme was found to give accurate solutions to both finite-dimensional and continuous constrained motion problems.

As an example of a real world problem, let us mention that a constrained motion problem for the SRMS (Shuttle Remote Manipulator System) was successfully solved with the described augmented Lagrangian method combined with the implicit time-integration algorithm. The problem was to geometrically constrain the motion of the end-effector of the space shuttle's robotic arm, and the algorithm was incorporated in the existing software for simulating the dynamics of the SRMS, see [10] for more details and further numerical experiments.

Acknowledgements

We would like to acknowledge the helpful comments and suggestions of the referee and of J.F. Bourgat, E.J. Dean, Y.M. Kuo, G. Nasser, and P. Le Tallec. The support of the following corporations and

institutions is also acknowledged: NASA and Lockheed Engineering and Sciences Company (Contract NAS 9-17900), University of Houston, and the Texas Board of Higher Education (Grants 003652091 ARP and 003652146 ATP).

References

1. Antman, S.S.: Multiple equilibrium states of nonlinearly elastic strings. SIAM J. Appl. Math. 37: 588–604 (1979).
2. Arora, J.S., Chahande, A.L., Paeng, J.K.: Multiplier methods for engineering optimization. Int. J. Numer. Methods Eng. 32: 1485–1525 (1991).
3. Bourgat, J.F., Dumay, J.M., Glowinski, R.: Large displacement calculations of flexible pipe-lines by finite element and non-linear programming methods. In: Oden, J.T. (ed.): Computational methods in nonlinear mechanics. North-Holland, Amsterdam, pp. 109–175 (1980).
4. Dean, E., Glowinski, R., Kuo, Y., Nasser, M.G.: On the discretization of some second order in time differential equations: applications to nonlinear wave problems. In: Balakrishnan, A.V. (ed.): Proceedings of the NASA-UCLA Workshop on Computational Techniques in Identification and Control of Flexible Flight Structures, Optimization Software, Los Angeles, pp. 199–246 (1990).
5. Gill, P.E., Murray, W., Wright, M.H.: Practical optimization. Academic Press, New York (1981).
6. Glowinski, R.: Numerical methods for nonlinear variational problems. Springer, Berlin Heidelberg New York Tokyo (1984).
7. Glowinski, R., Le Tallec, P.: Augmented Lagrangian and operator-splitting methods in nonlinear mechanics. SIAM, Philadelphia (SIAM studies in applied mathematics, vol. 9) (1989).
8. Hairer, E., Wanner, G.: Solving ordinary differential equations, vol. 2, stiff and differential-algebraic problems. Springer, Berlin Heidelberg New York Tokyo (Springer series in computational mathematics, vol. 14) (1991).
9. Hestenes, M.R.: Multiplier and gradient methods. J. Optim. Theory Appl. 4: 303–320 (1969).
10. Holmström, M.: Constrained motion problems with applications. Master's thesis, Department of Mechanical Engineering, University of Houston, Houston, Texas, U.S.A. (1993).
11. Lubich, C.: Extrapolation integrators for constrained multibody systems. Impact Comput. Sci. Eng. 3: 213–234 (1991).
12. Powell, M.J.D.: A method for nonlinear constraints in minimization problems. In: Fletcher, R. (ed.): Optimization. Academic Press, New York, pp. 283–298 (1969).
13. Rockafellar, R.T.: Lagrange multipliers and optimality. SIAM Rev. 35: 183–238 (1993).
14. Simeon, B., Führer, C., Rentrop, P.: Differential-algebraic equations in vehicle system dynamics. Surv. Math. Ind. 1: 1–37 (1991).

Authors' addresses: Dr. R. Glowinski, Department of Mathematics, University of Houston, Houston, TX 77204-3476, U.S.A. — M. Holmström, Department of Scientific Computing, University of Uppsala, Uppsala, Sweden.